



Published in final edited form as:

Cardiovasc Eng Technol. 2014 March 1; 5(1): 119–131. doi:10.1007/s13239-013-0167-1.

Cardiac fibroblast-derived 3D extracellular matrix seeded with mesenchymal stem cells as a novel device to transfer cells to the ischemic myocardium

Eric G. Schmuck, PhD¹, Jacob D. Mulligan, PhD¹, Rebecca L. Ertel, BS¹, Nicholas A. Kouris, PhD², Brenda M. Ogle, PhD², Amish N. Raval, MD^{1,2}, and Kurt W. Saupe, PhD^{1,†}

¹Department of Medicine, University of Wisconsin at Madison, Madison, WI 53706, USA

²Department of Biomedical Engineering, University of Wisconsin at Madison, Madison, WI 53706, USA

Abstract

Purpose—Demonstrate a novel manufacturing method to generate extracellular matrix scaffolds from cardiac fibroblasts (CF-ECM) as a therapeutic mesenchymal stem cell-transfer device.

Materials and Methods—Rat CF were cultured at high-density ($\sim 1.6 \times 10^5/\text{cm}^2$) for 10–14 days. Cell sheets were removed from the culture dish by incubation with EDTA and decellularized with water and peracetic acid. CF-ECM was characterized by mass spectrometry, immunofluorescence and scanning electron microscopy. CF-ECM seeded with human embryonic stem cell derived mesenchymal stromal cells (hEMSCs) were transferred into a mouse myocardial infarction model. 48 hours later, mouse hearts were excised and examined for CF-ECM scaffold retention and cell transfer.

Results—CF-ECM scaffolds are composed of fibronectin (82%), collagens type I (13%), type III (3.4%), type V (0.2%), type II (0.1%) elastin (1.3%) and 18 non-structural bioactive molecules. Scaffolds remained intact on the mouse heart for 48 hours without the use of sutures or glue. Identified hEMSCs were distributed from the epicardium to the endocardium.

Conclusions—High density cardiac fibroblast culture can be used to generate CF-ECM scaffolds. CF-ECM scaffolds seeded with hEMSCs can be maintained on the heart without suture or glue. hEMSC are successfully delivered throughout the myocardium.

Keywords

Cardiac Fibroblast; Extracellular Matrix; Stem Cell; Cardiac; Regeneration; Heart Failure; Myocardial Infarction

Corresponding Author: Eric G. Schmuck PhD, H6/385 Clinical Science Center, 600 Highland Ave, Madison, WI 53792, Phone: 608-263-9449, Fax: 608-263-0405, egs@medicine.wisc.edu.

[†]Died June 23rd, 2012

Conflict of Interest

Author ES, Author JM, Author RE, Author NK, Author BO, Author AR, and Author KS declare that they have no conflict of interest.

Animal Studies

All institutional and national guidelines for the care and use of laboratory animals were followed and approved by the University of Wisconsin Madison animal care and use committee.

Introduction

Heart failure (HF) continues to be a major public health challenge in the United States and worldwide. The incidence of HF in the United States is estimated at over 6.6 million people. HF is the leading reason for hospitalization and accounts for more than 280,000 deaths annually [1]. Ischemic heart disease is the most common underlying cause of HF [2]. Conventional management for ischemic HF aims to block neuro-hormonal factors through medical therapy and improve myocardial perfusion through surgical or percutaneous revascularization. However, a ceiling exists on the effectiveness of these therapies, as they improve cardiac function but do not restore lost or damaged tissue. Cell-based therapies are widely being tested to treat refractory ischemic HF but clinical trials have shown only modest benefit [3–13]. Cell delivery methods include intravenous infusion, intracoronary infusion and direct intramuscular injection; however, these offer low acute cell retention within the myocardium [14–20]. Alternatively, an ECM scaffold that is seeded with cardio-reparative progenitor cells and applied directly to the myocardium may improve local cell retention and potentially enhance the therapeutic effect.

Numerous ECM scaffolds are being investigated as stem cell delivery devices for cardiac indications. There are over 28 scaffolds commercially available which are broadly categorized as synthetic materials [21] [22, 23] and naturally occurring biomaterials such as ECM obtained from decellularization of heart valves [24–26], skeletal muscle [27], human or bovine dermis [28, 21], and porcine small intestine [21, 29, 30]. In addition, manufactured collagen based ECM sponge materials [31, 32] and cell sheets including MSCs [33–35] fibroblasts [36, 35], myoblasts [35, 37] and cardiomyocytes [35, 38] have been studied. Typically, ECM scaffolds are surgically positioned on the surface of the heart using glues or sutures. While these studies generally demonstrate benefit in pre-clinical models, the optimal ECM remains unknown [39, 32, 31, 40, 35]. Herein, we demonstrate a novel and reliable manufacturing method for an ECM scaffold derived from cardiac fibroblasts that can transfer mesenchymal stem cells to the ischemic myocardium, without the need for sutures or glues.

Materials and Methods

Manufacturing the Cardiac Fibroblast derived Extracellular Matrix (CF-ECM)

Rat cardiac fibroblasts were isolated using previously described methods [41, 42]. Briefly, male Lewis rats (260–400g) were sacrificed by CO₂ asphyxiation, hearts rapidly excised, atria removed and ventricles placed into ice cold PBS with 1% penicillin/streptomycin. Hearts were finely minced then placed into 10 mL digestion media (Dulbecco's Modified Eagle's Medium (DMEM), 73 U/mL collagenase 2, 2 µg/mL pancreatin (4×)) and incubated at 37°C with agitation for 35 min. The digest mixture was centrifuged at 1000×g for 20 min at 4°C. The resulting cell pellet was suspended in 10 mL of fresh digestion media and incubated at 37°C with agitation for 30 minutes. The resulting digest was sieved through a 70 µm cell strainer and digest solution diluted with 10 mL of culture media (DMEM, 10% Fetal Bovine Serum (FBS), 1% penicillin/streptomycin). The cell suspension was then centrifuged at 1000×g for 20 min at 4°C. The cell pellet was suspended in 16 mL culture media and plated into two T75 culture flasks (8 mL per flask). The cells were allowed to attach under standard culture conditions (37°C, 5% CO₂, 100% humidity) for 2 hours, then non-adherent cells removed by washing with PBS, and culture media replaced. Primary cardiac fibroblast cultures were typically confluent in 4–7 days.

To induce CF-ECM scaffold formation, cardiac fibroblasts from passage 2–3 were plated at a density of approximately 1.1×10^5 to 2.2×10^5 per cm² in high glucose DMEM + 10% FBS and 1% penicillin/streptomycin and cultured at 37°C, 5% CO₂ and 100% humidity for 10 to

14 days. The combined cardiac fibroblasts and extracellular matrix were removed from the culture dish by incubation with 2 mM EDTA solution at 37°C. The resulting cardiac fibroblast cell sheet was then denuded of cells by incubation with molecular grade water followed by incubation with 0.15% peracetic acid (PAA buffer) for 24–48 hours at 4°C with constant agitation. Peracetic acid has been established as an effective decellularizing agent without obvious deleterious effects on proteins structure, composition or physical characteristics [43]. The resulting matrix was then rinsed repeatedly with sterile water followed by PBS (Figure 1A and 1B).

Characterization of CF-ECM

CF-ECM scaffold protein composition and structure was characterized by mass spectrometry, confocal microscopy and scanning electron microscopy.

Mass Spectrometry—All solutions were prepared fresh just prior to use with HPLC grade water. CF-ECM scaffolds were suspended in 15 μ L 8M urea and then 20 μ L of 0.2% ProteaseMax™ added. The CF-ECM was then dissolved into solution by vortexing and pipetting. A volume of 58.5 μ L of 50 mM NH_4HCO_3 was added to a final volume of 93.5 μ L. The sample was then reduced by adding 1 μ L of 0.5 M DTT and incubating at 56°C for 20 minutes. 2.7 μ L of 0.55 M iodoacetamide was added and incubated for 15 minutes at room temperature in the dark. 1 μ L of 1% ProteaseMax™ and 2 μ L of 1 μ g/ μ L Trypsin Gold™ were added and incubated overnight at 37°C. The following day 0.5 μ L of trifluoroacetic acid was added to the final concentration of 0.5% to stop the reaction. The sample was then centrifuged at 14,000 \times g for 10 minutes at 4°C. 2 μ L of sample was injected onto an Eksigent 2D nanoLC chromatography system and eluted into a Thermo Finnigan LTQ Mass Spectrometer. The sample was retained on an Agilent Zorbax SB300-C8 trap and eluted by reverse phase gradient onto a 0.100 mm \times 100 mm emitter packed in-house with 5 μ m bead 300 Å pore MagicC18 material. Mobile phase solution consisted of a water and 0.1% formic acid aqueous phase and a 0.1% formic acid in 50% acetonitrile:ethanol organic phase. The gradient ran from 1 to 60 min and from 5 to 35% organic with a 95% wash. Eluent was ionized by a positive 3000 V nanoESI and analyzed by a Data Dependent triple play template. The top 5 m/z were selected by intensity, charge state was analyzed by zoom scan, and MS/MS were performed with wideband activation, dynamic exclusion of 1 for 60 s with a list of 300 m/z and a width of \pm 1.5/0.5m/z, collision energy of 35%, and noise level of 3000NL. Sequest searches were performed via Bioworks 3.0 using a downloaded Swissprot database for Rat (Oct 2010) and its reversed sequences. Search parameters included trypsin digestion, 1 missed cleavage, amino acid length of 6 to 100 with tolerance of 1.4 da, dynamic modifications of methionine methylation (+14 da) and cysteine carboxyamidomethylation (+57 da). Results were filtered to less than 5% false discovery rate, defined by number of proteins identified with reversed sequences divided by the total number proteins identified minus reversed number, and multiplied by 100 [44].

Confocal Microscopy—CF-ECM scaffolds were fixed in fresh 3.6% paraformaldehyde, embedded in paraffin and sectioned in 5 μ m sections and mounted on slides. De-paraffinized and rehydrated slides were incubated with 0.1% trypsin and sodium citrate heat retrieval was performed by incubation in 10 mM sodium citrate, 0.05% Tween-20 buffer pH 6 for 60 minutes in an Oster® rice steamer (95–100°C). Slides were blocked with 1% bovine serum albumin in PBST for 1 hour at room temperature then incubated with primary antibodies (all antibodies purchased from Santa Cruz Biotechnology) at a dilution of 1:50 and incubated at 37°C for 1 hour. Slides were then washed in PBST and incubated in secondary antibodies at 1:1000 dilution in 1% bovine serum albumin in PBST (all secondary antibodies purchased from Invitrogen) for 1 hour at room temperature in the dark. Slides were washed in PBST and counter stained with 1 μ g/mL DAPI for 10 minutes then cover slips mounted with

aqueous mounting media and the edges sealed with quick dry, clear nail polish. Slides were imaged at the W.M Keck Laboratory for Biological Imaging with a Nikon A1R scanning confocal microscope or a Leica TCS SP5 II confocal microscope.

Scanning Electron Microscopy—Sample preparation and imaging was carried out by the Biological and Biomaterials Preparation, Imaging, and Characterization Facility at University of Wisconsin Madison. Briefly, ECM scaffold samples were diced with a double sided razor blade to approximately 3 mm² then fixed in 1% paraformaldehyde, 2% glutaraldehyde in 0.1M sodium cacodylate buffer overnight at 4°C. Samples were washed twice in molecular grade water then secondary fixation carried out by incubated with 1% osmium tetroxide (in water) for 30 minutes. Samples were washed twice in molecular grade water then dehydrated with a series of 10 minute ethanol incubations (30, 50, 70, 75, 80, 90, 95, and 100%) and sieve dried. Samples were then critical point dried in a Tousimis Samdri 780 four times and ion beam sputter coated with 2.5 nm of platinum. Finally, the prepared samples were imaged on a Hitachi S900 High Resolution Field Emission Microscope.

CF-ECM scaffold to transfer stem cells *in vivo* to the ischemic myocardium

Myocardial Infarction Model—A mouse model of myocardial infarction (MI) using a surgical left anterior descending coronary artery ligation was used to demonstrate the feasibility of CF-ECM application [45]. Immunocompetent C57Bl/6 mice were purchased from Harlan Laboratories and all procedures were carried out in accordance with protocols approved by the Institutional Animal Care and Use Committee. Following induction of isoflurane anesthesia (3%), the mouse was intubated with an 18 gauge catheter and placed on a mouse ventilator at 120–130 breaths per minute with a stroke volume of 150 µL and maintained on 2% isoflurane. A left lateral incision through the fourth intercostal space was made to expose the heart. After visualizing the left anterior descending coronary artery, a 7-0 or 8-0 Prolene suture was placed through the myocardium in the anterolateral wall and secured as previously described [45, 46]. Coronary artery entrapment was confirmed by observing blanching of the distal circulation at the ventricular apex. Absorbable sutures were used to close the ribs and muscle layers. The overlying skin was closed by additional 6-0 nylon or silk sutures, after which mice were recovered.

H9 human embryonic stem cell derived mesenchymal stromal cells (hEMSC) passage 7 were isolated and expanded to demonstrate the feasibility of CF-ECM scaffold stem cell delivery. Details on the derivation and characterization of these cells are found in reference [47]. Twenty-four hours post infarction, the mouse was re-anesthetized and the chest reopened for scaffold placement. CF-ECM scaffolds were seeded with 7.5×10^5 hEMSCs and incubated for 2 hours prior to transfer to the epicardial surface of the MI area. The CF-ECM scaffold plus hEMSC were manually transferred and adjusted onto the epicardial surface of the beating heart using surgical forceps. The chest was left open for 15 min to observe for any gaping or sliding between the scaffold and heart. Thereafter, the chest was closed and the animal was recovered. Forty-eight hours after hEMSC loaded CF-ECM was placed, mice were sacrificed and the hearts were examined.

Biodistribution of CF-ECM scaffold-delivered hEMSCs in the myocardium

hEMSC biodistribution was assessed by 3-dimensional whole heart imaging tracking for green fluorescent protein expression and by Fluorescence *In Situ* Hybridization (FISH) tracking for human centromeres.

3-dimensional whole heart imaging for EGFP+ hEMSCs—Human ESC lines H9 Cre-LoxP (constitutive EGFP expression) were obtained from WiCell (Madison, WI) at passage 22. Cells were cultured in mTeSR1 medium (StemCell Technologies) on Matrigel

(BD Biosciences) coated flasks for 3–4 passages without removing differentiated areas. Differentiated cells were isolated and cultured in MSC growth medium (10% MSC characterized FBS, MEM non-essential amino acids, alpha-MEM) on tissue culture plastic until all cells had a fibroblast-like morphology. EGFP+hESMSC exhibited the following flow cytometry profile: CD14–, CD31–, CD34–, CD45–, CD73+, CD90+ and CD105+ and could differentiate into adipocytes, chondrocytes and osteocytes.

A male Lewis rat underwent myocardial infarction using the coronary left anterior descending coronary artery ligation model as described above. Twenty four hours post infarction, a CF-ECM scaffold was seeded with 7.5×10^5 EGFP+ hEMSCs for 2 hours prior to transfer to the peri-infarct region. Twenty-four hours after stem cell transfer, the heart was excised and frozen in a cryo-imaging embedding compound (BioInVision, Cleveland OH). The entire heart was then imaged in successive 20 mm slices with confocal (Long Pass GFP filter) and bright field microscopy on an Olympus MVX-10 1X microscope at 0.63 \times magnification.. The scan field was 22.796 mm \times 16.514 mm and pixel size of 10.232 microns. Co-registered bright field and confocal images were reconstructed to generate a 3-dimensional whole heart volume.

Fluorescence In Situ Hybridization (FISH)—A commercial FISH kit was used for hEMSC tracking within the mouse myocardium (Kreatech KBI-60007). Mouse hearts were rapidly excised, fixed in 3.7% paraformaldehyde for 24 hours and embedded in paraffin. Short access 5 micron sections of the heart were mounted on pro-bond slides. Slides were de-paraffinized by baking at 56°C for 4 hours, followed by xylene incubation. Slides were rehydrated by ethanol series, followed by incubation in 96–98°C Pretreatment Solution A, then rinsed in water and digested with 200 μ L Pepsin Solution for 50 minutes at room temperature. Digestion was stopped by rinsing in water and incubating in 2 X SSC buffer at room temp. Slides were dehydrated and 10 μ L All Human Centromere Probe (Kreatech KI-20000R) applied to the sample, sealed with a cover slip and incubated at 80°C for 5 minutes. Slides were then incubated overnight at 37°C. Slides were washed in Wash buffer II and the cover slip removed then washed in Wash buffer I at 72°C. Finally, the slides were washed in Wash buffer II, dehydrated and allowed to air dry. Slides were counterstained with DAPI and a cover slip mounted. Analysis was performed on a Leica TCS SP5 II confocal microscope. One heart slice per animal was scanned in entirety and the number of cells and distance migrated from the epicardium quantified.

Results

CF-ECM Scaffold Manufacturing and Protein Characterization

Over 500 CF-ECM scaffolds were successfully and reliably generated during development and over the course of these studies. For this report, scaffold production was carried out in circular 40 mm dishes resulting in CF-ECM scaffolds of 15–20 mm in diameter (Figure 1A). Thickness of the CF-ECM scaffolds varied 50 to >150 μ m and was primarily dependent on cardiac fibroblast seeding density. Seeding densities tested ranged from $<5.5 \times 10^4$ to greater than $>2.2 \times 10^5$ cells per cm^2 . Seeding densities of $<5.5 \times 10^4$ cells/ cm^2 failed to generate scaffolds while exceeding 2.2×10^5 cells per cm^2 resulted in premature release of cardiac fibroblasts from the culture dish. We tested length of culture from 7 days to 21 days and found that 10–14 days produced the most consistent ECM scaffold. If cardiac fibroblasts were cultured for <10 or >14 days, the resulting scaffold, if it formed, was thin and fragile.

Protein Composition—CF-ECM scaffolds derived from four different cardiac fibroblast lines were analyzed. Normalized spectral abundance factor (NSAF) was used to quantify the abundance of structural extracellular matrix proteins (Figure 2D). Fibronectin (82.1 +/-

2.2%) was found to be the primary component of CF-ECM with collagen type I (6.7 +/- 0.9% collagen 1A1 and 6.0 +/- 0.7% collagen 1A2) and collagen type III (3.4 +/- 0.08%) accounting for a lesser proportion of the matrix. Additionally, small amounts of elastin (1.3 +/- 0.5%), collagen types II (0.1 +/- 0.007%), V (0.2 +/- 0.06%) and XI (0.2 +/- 0.2%) were detected. Additionally, 18 bioactive molecules were identified but could not be reliably quantified due to low levels (Figure 2E).

Imaging confirmed that the CF-ECM scaffold was composed of mostly fibronectin as well as smaller amounts of collagen type I, which primarily localized to the surface of the matrix. Decellularization was confirmed by the absence of DAPI stained nuclei. High resolution imaging of the surface of the CF-ECM scaffold using scanning electron microscopy revealed a honeycomb like architecture with occasional residual cardiac fibroblast cell membrane material (Figure 2A–C).

Feasibility of CF-ECM as a cell transfer device to the ischemic myocardium

A myocardial infarction (MI) model was created in 11 mice. An additional 5 control mice underwent sham thoracotomy. Premature death occurred due to the thoracotomy with MI in 3 mice, and due to the thoracotomy in 2 of the control mice. Therefore, the results of the remaining 11 mice which survived to treatment are presented (3 shams, 8 MI). Following therapeutic transfer, the CF-ECM plus hEMSCs could be easily positioned and adjusted onto the ischemic area of the left ventricle, without gaps, sliding or tearing in all animals. Lung color, right ventricular performance, left ventricular performance and inferior vena cava dimension were visibly unchanged, suggesting no acute left ventricular constriction (supplemental video 1, Figure 3A). Forty-eight hours after treatment, the scaffold remained adherent to the epicardial heart surface in approximately the same position as they were placed (Figure 3B). Close scaffold adherence to the epicardium was confirmed by hematoxylin and eosin stain (Figure 3C) and immunofluorescent stain for fibronectin (Figure 3D).

3-D co-registered bright field and confocal whole heart imaging 24 hours after scaffold placement showed adherence of the scaffold without gaps or tears, and no distortion of the underlying myocardium. At this early time period, EGFP+ hEMSC cells were detected predominantly within the CF-ECM scaffold and the epicardium beneath the scaffold (Figure 4A – C, and supplemental video 2).

Using FISH, hEMSCs were detectable in the scaffold after 48 hours (Figure 5A–C). hEMSCs were successfully transferred to the myocardium in 7 of 8 animals in the MI group, and 2 of 3 animals in the sham control group. In all 9 animals where stem cell transfer had occurred, hEMSCs were detected scattered within the epicardial surface and mid-myocardium underlying the scaffold, with the largest fraction being within the epicardium. Of note, hEMSCs were detected >500 μ m from the scaffold in two animals one in the MI and one in the sham group (Figure 5D). No differences were detected in hEMSC transfer between sham and MI animals.

Discussion

We have demonstrated a novel and reliable manufacturing method to generate CF-ECM scaffolds that can transfer MSCs to the ischemic myocardium. The CF-ECM stem cell delivery scaffold does not require sutures or glues, does not appear to acutely impair ventricular filling, does not cause acute toxicity, and has a cardiac derived matrix protein composition that is homologous to the recipient myocardium.

Our CF-ECM manufacturing method is simple, scalable and potentially transferable for clinical applications. Human cardiac fibroblasts are commercially available, highly proliferative and amenable to culture in large format cell production vessels (i.e. Bioreactors). This is important as large numbers of fibroblasts will be necessary for clinical scale production of CF-ECM. Additionally, with the commercial availability of cardiac fibroblasts, CF-ECM has the potential to be manufactured as an “off the shelf” allogeneic cell delivery tool or could be personalized by collecting cardiac biopsies and isolating cardiac fibroblasts from individual patients to create an autologous cell delivery tool. Customization of the CF-ECM size and shape may be important when delivering therapeutic stem cells to the site of myocardial injury. Such parameters can be manipulated by simply altering the size and shape of the culture vessel as well as trimming the CF-ECM to a desired size and or shape.

ECM appears to provide more than just the structural support for organs and tissue. It is now widely accepted that organ-specific ECM is synthesized by local fibroblasts to produce unique combinations of tissue-specific structural proteins and bioactive molecules such as growth factors [48–52]. It is also a key factor for cell attachment, survival, proliferation, migration and differentiation [53, 52]. A cardiac fibroblast-derived ECM that can deliver stem cells may offer unique benefits for cardiac disease applications. For example, the protein composition of our CF-ECM scaffold appears similar to post MI healing myocardium, which in humans has been shown to be enriched for fibronectin for up to 28 days post MI [54]. Fibronectin has been shown to recruit endogenous cardiac progenitor cells following MI [55] and to induce cell proliferation, adhesion, survival and angiogenesis [56, 57]. In addition, fibronectin is an adhesive protein due to the expression of multiple binding sites for collagen, fibrin/fibronectin, vitronectin, heparin and cells through a variety of cell surface integrins [58, 59].

One important aspect of CF-ECM is the incorporation of bioactive molecules. We detected 18 bioactive molecules including growth factors and cytokines that are involved in important cellular functions such as adhesion, de-adhesion, proliferation and differentiation [53, 60]. For example, transforming growth factor beta ($TGF-\beta_{I-III}$) is bound to collagen and fibronectin in a latent form and activated by high heat, pH extremes, proteases, chaotropic agents, integrins and thrombospondin 1 [61]. Following MI, the TGF- β family have been shown to be involved in regulating cardiac healing, by exerting pleiotropic effects on inflammatory immune cells, cardiac fibroblasts and cardiomyocytes [62]. Galectin-1 has been shown to reduce acute inflammation and trigger alternative activation of macrophages (M2) [63] while Galectin-3 induces neutrophil adhesion and activation as well as being a chemo-attractant of monocytes/macrophages [64, 65]. Secreted protein, acidic and rich in cysteine or SPARC mediates early ECM remodeling following MI [66] and has been shown to increase fibronectin content in the myocardium, which may increase the recruitment of endogenous stem cells to the area [66, 55]. Finally, Biglycan, a small pericellular matrix proteoglycan, has been shown to be required for the formation of a stable collagen network and stabilization of hemodynamics following MI [67]. Many of the bioactive molecules detected in CF-ECM are pleiotropic and their precise effects under the dynamic infarction conditions are difficult to predict; however, they likely play a beneficial role in post MI remodeling and early stabilization of the infarcted tissue.

Our CF-ECM decellularization process does not employ chemical crosslinking which has implications for healing and immune response [68, 69]. The effects of chemical crosslinking of bioscaffolds may be potentially detrimental to the tissue healing [70]. Conversely, recent studies have shown that ECM scaffolds that are not chemically cross-linked promote the infiltration and activation of anti-inflammatory macrophages (M2) [68, 69, 71]. M2 macrophages are associated with beneficial immune-regulatory, remodeling, matrix

deposition and graft acceptance [68, 69]. Future studies will focus on the immune response to CF-ECM specifically the M2 macrophage population within the myocardium and the CF-ECM.

Clinical trials evaluating the safety and efficacy of stem cells therapy for ischemic heart disease have suggested that the various delivery approaches are safe; however, treatment efficacy in terms of improved cardiac function has been mixed [4–13]. A potential reason may be poor transplanted stem cell retention. Stem cells have been delivered through intravenous (IV), intracoronary (IC), interstitial retrograde coronary venous (IRCV) and intramuscular (IM) injections. Acute cell retention for these delivery approaches have ranged from 20% to <1% within a few hours of delivery [20, 72, 73] [74]. Vascular or lymphatic wash out or egress, immune rejection, and hostile environment are among the potential reasons for this observation. Implantable epicardial scaffolds, and our CF-ECM in particular, may improve transferred stem cell retention by providing a hospitable platform from which stem cells gradually infiltrate the ischemic myocardium [75, 76].

Currently available biomaterials require suture and or glue to affix the material to the heart [32, 39, 77–79, 31, 30, 80]. The use of suture may increase damage to the heart and risk perforation; while glues may reduce the permeation of homing signals to the cells in the materials reducing the drive for cells to home to injured tissue. Thus, CF-ECMs unique property of self-attachment to the heart creating a platform from which cells can freely home to injured tissues, while not risking additional cardiac injury, is unique in the field. In this study, we did not test the specific nature of this attachment, but we speculate it is initially due to surface tension while long term attachment may be mediated by fibronectin as described above. We found that hEMSCs were preserved in the scaffold at 24 and 48 hours with cells migrating deep within the myocardium by 48 hours post scaffold placement. Cell migration was observed in the acutely injured and the uninjured myocardium, suggesting that CF-ECM stem cell transfer is applicable for both acute and chronic cardiac ischemia conditions.

Several limitations should be acknowledged. This report is primarily intended to demonstrate a new manufacturing method for deriving cardiac ECM scaffolds that can safely deliver stem cells to the ischemic myocardium. Therapeutic efficacy of our CF-ECM stem cell transfer approach or a scaffold only approach cannot be extrapolated based on this data. In addition, our results are limited to short term retention up to 48 hours, although local retention efficiency with CF-ECM scaffold stem cell transfer appears to be higher than published results of other infusion or intramyocardial injection approaches. Finally, the CF-ECM scaffold was produced using rat cardiac fibroblasts. For clinical translation, future work will attempt to demonstrate similar manufacturing methods and scaffold properties using human cardiac fibroblasts.

Conclusion

We have demonstrated a new manufacturing method and characterized the protein composition of a clinically translatable CF-ECM scaffold capable of efficient acute transfer of mesenchymal stem cells in a pre-clinical model of ischemic myocardium. Future studies are required to demonstrate therapeutic efficacy of this approach.

Supplementary Material

Refer to Web version on PubMed Central for supplementary material.

Acknowledgments

This study was supported by the National Heart, Lung, and Blood Institute grant number 1R21HL092477 and the National Institutes of Health, under Ruth L. Kirschstein National Research Service Award T32 HL 07936 from the National Heart Lung and Blood Institute to the University of Wisconsin-Madison Cardiovascular Research Center.

References

1. Roger VL, Go AS, Lloyd-Jones DM, Benjamin EJ, Berry JD, Borden WB, et al. Heart disease and stroke statistics--2012 update: a report from the American Heart Association. *Circulation*. 2012; 125(1):e2–e220.10.1161/CIR.0b013e31823ac046 [PubMed: 22179539]
2. Kalogeropoulos A, Georgiopoulou V, Kritchevsky SB, Psaty BM, Smith NL, Newman AB, et al. Epidemiology of incident heart failure in a contemporary elderly cohort: the health, aging, and body composition study. *Archives of internal medicine*. 2009; 169(7):708–15.10.1001/archinternmed.2009.40 [PubMed: 19365001]
3. Abdel-Latif A, Bolli R, Tleyjeh IM, Montori VM, Perin EC, Hornung CA, et al. Adult bone marrow-derived cells for cardiac repair: a systematic review and meta-analysis. *Archives of internal medicine*. 2007; 167(10):989–97. 167/10/989 [pii]. 10.1001/archinte.167.10.989 [PubMed: 17533201]
4. Schachinger V, Erbs S, Elsasser A, Haberbosch W, Hambrecht R, Holschermann H, et al. Intracoronary bone marrow-derived progenitor cells in acute myocardial infarction. *N Engl J Med*. 2006; 355(12):1210–21. [PubMed: 16990384]
5. Meyer GP, Wollert KC, Lotz J, Steffens J, Lippolt P, Fichtner S, et al. Intracoronary bone marrow cell transfer after myocardial infarction: eighteen months' follow-up data from the randomized, controlled BOOST (BOne marrOw transfer to enhance ST-elevation infarct regeneration) trial. *Circulation*. 2006; 113(10):1287–94. [PubMed: 16520413]
6. Meyer GP, Wollert KC, Lotz J, Pirr J, Rager U, Lippolt P, et al. Intracoronary bone marrow cell transfer after myocardial infarction: 5-year follow-up from the randomized-controlled BOOST trial. *Eur Heart J*. 2009; 30(24):2978–84. ehp374 [pii]. 10.1093/eurheartj/ehp374 [PubMed: 19773226]
7. Janssens S, Dubois C, Bogaert J, Theunissen K, Deroose C, Desmet W, et al. Autologous bone marrow-derived stem-cell transfer in patients with ST-segment elevation myocardial infarction: double-blind, randomised controlled trial. *Lancet*. 2006; 367(9505):113–21. [PubMed: 16413875]
8. Menasche P, Alfieri O, Janssens S, McKenna W, Reichenspurner H, Trinquart L, et al. The Myoblast Autologous Grafting in Ischemic Cardiomyopathy (MAGIC) trial: first randomized placebo-controlled study of myoblast transplantation. *Circulation*. 2008; 117(9):1189–200.10.1161/CIRCULATIONAHA.107.734103 [PubMed: 18285565]
9. Hare JM, Fishman JE, Gerstenblith G, Difeo Velazquez DL, Zambrano JP, Suncion VY, et al. Comparison of Allogeneic vs Autologous Bone Marrow-Derived Mesenchymal Stem Cells Delivered by Transendocardial Injection in Patients With Ischemic Cardiomyopathy: The POSEIDON Randomized Trial. *JAMA : the journal of the American Medical Association*. 2012;1–11. 10.1001/jama.2012.25321 1388858. [pii].
10. Hare JM, Traverse JH, Henry TD, Dib N, Strumpf RK, Schulman SP, et al. A randomized, double-blind, placebo-controlled, dose-escalation study of intravenous adult human mesenchymal stem cells (prochymal) after acute myocardial infarction. *J Am Coll Cardiol*. 2009; 54(24):2277–86. [PubMed: 19958962]
11. Bolli R, Chugh AR, D'Amario D, Loughran JH, Stoddard MF, Ikram S, et al. Cardiac stem cells in patients with ischaemic cardiomyopathy (SCIPIO): initial results of a randomised phase 1 trial. *Lancet*. 2011; 378(9806):1847–57.10.1016/S0140-6736(11)61590-0 [PubMed: 22088800]
12. Makkar RR, Smith RR, Cheng K, Malliaras K, Thomson LE, Berman D, et al. Intracoronary cardiosphere-derived cells for heart regeneration after myocardial infarction (CADUCEUS): a prospective, randomised phase 1 trial. *Lancet*. 2012; 379(9819):895–904.10.1016/S0140-6736(12)60195-0 [PubMed: 22336189]
13. Schaefer A, Zwadlo C, Fuchs M, Meyer GP, Lippolt P, Wollert KC, et al. Long-term effects of intracoronary bone marrow cell transfer on diastolic function in patients after acute myocardial infarction: 5-year results from the randomized-controlled BOOST trial--an echocardiographic

- study. *Eur J Echocardiogr.* 2010; 11(2):165–71. jep191 [pii]. 10.1093/ejehocard/jep191 [PubMed: 19946118]
14. Qian H, Yang Y, Huang J, Gao R, Dou K, Yang G, et al. Intracoronary delivery of autologous bone marrow mononuclear cells radiolabeled by 18F-fluoro-deoxy-glucose: tissue distribution and impact on post-infarct swine hearts. *J Cell Biochem.* 2007; 102(1):64–74. [PubMed: 17407141]
 15. Forest VF, Tirouvanziam AM, Perigaud C, Fernandes S, Fusellier MS, Desfontis JC, et al. Cell distribution after intracoronary bone marrow stem cell delivery in damaged and undamaged myocardium: implications for clinical trials. *Stem Cell Res Ther.* 2010; 1(1):4. [PubMed: 20504285]
 16. Muller-Ehmsen J, Whittaker P, Kloner RA, Dow JS, Sakoda T, Long TI, et al. Survival and development of neonatal rat cardiomyocytes transplanted into adult myocardium. *J Mol Cell Cardiol.* 2002; 34(2):107–16. [PubMed: 11851351]
 17. Mirotsov M, Zhang Z, Deb A, Zhang L, Gnechchi M, Noiseux N, et al. Secreted frizzled related protein 2 (Sfrp2) is the key Akt-mesenchymal stem cell-released paracrine factor mediating myocardial survival and repair. *Proc Natl Acad Sci U S A.* 2007; 104(5):1643–8. 10.1073/pnas.0610024104 [PubMed: 17251350]
 18. Murry CE, Soonpaa MH, Reinecke H, Nakajima H, Nakajima HO, Rubart M, et al. Haematopoietic stem cells do not transdifferentiate into cardiac myocytes in myocardial infarcts. *Nature.* 2004; 428(6983):664–8. [PubMed: 15034593]
 19. Chimenti I, Smith RR, Li TS, Gerstenblith G, Messina E, Giacomello A, et al. Relative roles of direct regeneration versus paracrine effects of human cardiosphere-derived cells transplanted into infarcted mice. *Circ Res.* 2010; 106(5):971–80. [PubMed: 20110532]
 20. Hou D, Youssef E, Brinton T, Zhang P, Rogers P, Price E, et al. Radiolabeled cell distribution after intramyocardial, intracoronary, and interstitial retrograde coronary venous delivery: implications for current clinical trials. *Circulation.* 2005; 112(9 Suppl):I150–6. [PubMed: 16159808]
 21. Badylak SF, Freytes DO, Gilbert TW. Extracellular matrix as a biological scaffold material: Structure and function. *Acta Biomater.* 2009; 5(1):1–13. [PubMed: 18938117]
 22. Silva EA, Mooney DJ. Synthetic extracellular matrices for tissue engineering and regeneration. *Curr Top Dev Biol.* 2004; 64:181–205. [PubMed: 15563948]
 23. Ratner BD, Bryant SJ. Biomaterials: where we have been and where we are going. *Annu Rev Biomed Eng.* 2004; 6:41–75. [PubMed: 15255762]
 24. Bader A, Schilling T, Teebken OE, Brandes G, Herden T, Steinhoff G, et al. Tissue engineering of heart valves—human endothelial cell seeding of detergent acellularized porcine valves. *Eur J Cardiothorac Surg.* 1998; 14(3):279–84. [PubMed: 9761438]
 25. Booth C, Korossis SA, Wilcox HE, Watterson KG, Kearney JN, Fisher J, et al. Tissue engineering of cardiac valve prostheses I: development and histological characterization of an acellular porcine scaffold. *J Heart Valve Dis.* 2002; 11(4):457–62. [PubMed: 12150290]
 26. Korossis SA, Booth C, Wilcox HE, Watterson KG, Kearney JN, Fisher J, et al. Tissue engineering of cardiac valve prostheses II: biomechanical characterization of decellularized porcine aortic heart valves. *J Heart Valve Dis.* 2002; 11(4):463–71. [PubMed: 12150291]
 27. Borschel GH, Dennis RG, Kuzon WM Jr. Contractile skeletal muscle tissue-engineered on an acellular scaffold. *Plast Reconstr Surg.* 2004; 113(2):595–602. discussion 3–4. [PubMed: 14758222]
 28. Kouris NA, Schaefer JA, Hatta M, Freeman BT, Kamp TJ, Kawaoka Y, et al. Directed Fusion of Mesenchymal Stem Cells with Cardiomyocytes via VSV-G Facilitates Stem Cell Programming. *Stem cells international.* 2012; 2012:414038. 10.1155/2012/414038 [PubMed: 22701126]
 29. Hata H, Bar A, Dorfman S, Vukadinovic Z, Sawa Y, Haverich A, et al. Engineering a novel three-dimensional contractile myocardial patch with cell sheets and decellularised matrix. *Eur J Cardiothorac Surg.* 2010; 38(4):450–5. 10.1016/j.ejcts.2010.02.009 [PubMed: 20335044]
 30. Tan MY, Zhi W, Wei RQ, Huang YC, Zhou KP, Tan B, et al. Repair of infarcted myocardium using mesenchymal stem cell seeded small intestinal submucosa in rabbits. *Biomaterials.* 2009; 30(19):3234–40. 10.1016/j.biomaterials.2009.02.013 [PubMed: 19261327]

31. Chachques JC, Trainini JC, Lago N, Masoli OH, Barisani JL, Cortes-Morichetti M, et al. Myocardial assistance by grafting a new bioartificial upgraded myocardium (MAGNUM clinical trial): one year follow-up. *Cell Transplant*. 2007; 16(9):927–34. [PubMed: 18293891]
32. Cortes-Morichetti M, Frati G, Schussler O, Duong Van Huyen JP, Lauret E, Genovese JA, et al. Association between a cell-seeded collagen matrix and cellular cardiomyoplasty for myocardial support and regeneration. *Tissue Eng*. 2007; 13(11):2681–7.10.1089/ten.2006.0447 [PubMed: 17691866]
33. Hamdi H, Planat-Benard V, Bel A, Puymirat E, Geha R, Pidal L, et al. Epicardial adipose stem cell sheets results in greater post-infarction survival than intramyocardial injections. *Cardiovasc Res*. 2011
34. Masuda S, Shimizu T, Yamato M, Okano T. Cell sheet engineering for heart tissue repair. *Adv Drug Deliv Rev*. 2008; 60(2):277–85. [PubMed: 18006178]
35. Matsuura K, Haraguchi Y, Shimizu T, Okano T. Cell sheet transplantation for heart tissue repair. *Journal of controlled release : official journal of the Controlled Release Society*. 2013; 169(3): 336–40.10.1016/j.jconrel.2013.03.003 [PubMed: 23500057]
36. Kellar RS, Shepherd BR, Larson DF, Naughton GK, Williams SK. Cardiac patch constructed from human fibroblasts attenuates reduction in cardiac function after acute infarct. *Tissue Eng*. 2005; 11(11–12):1678–87. [PubMed: 16411813]
37. Miyagawa S, Saito A, Sakaguchi T, Yoshikawa Y, Yamauchi T, Imanishi Y, et al. Impaired myocardium regeneration with skeletal cell sheets--a preclinical trial for tissue-engineered regeneration therapy. *Transplantation*. 2010; 90(4):364–72.10.1097/TP.0b013e3181e6f201 [PubMed: 20555308]
38. Kawamura M, Miyagawa S, Miki K, Saito A, Fukushima S, Higuchi T, et al. Feasibility, safety, and therapeutic efficacy of human induced pluripotent stem cell-derived cardiomyocyte sheets in a porcine ischemic cardiomyopathy model. *Circulation*. 2012; 126(11 Suppl 1):S29–37.10.1161/CIRCULATIONAHA.111.084343 [PubMed: 22965990]
39. Giraud MN, Flueckiger R, Cook S, Ayuni E, Siepe M, Carrel T, et al. Long-term evaluation of myoblast seeded patches implanted on infarcted rat hearts. *Artificial organs*. 2010; 34(6):E184–92.10.1111/j.1525-1594.2009.00979.x [PubMed: 20482708]
40. Rane AA, Christman KL. Biomaterials for the treatment of myocardial infarction: a 5-year update. *J Am Coll Cardiol*. 2011; 58(25):2615–29.10.1016/j.jacc.2011.11.001 [PubMed: 22152947]
41. Dubey RK, Gillespie DG, Mi Z, Jackson EK. Exogenous and endogenous adenosine inhibits fetal calf serum-induced growth of rat cardiac fibroblasts: role of A2B receptors. *Circulation*. 1997; 96(8):2656–66. [PubMed: 9355907]
42. Baharvand H, Azarnia M, Parivar K, Ashtiani SK. The effect of extracellular matrix on embryonic stem cell-derived cardiomyocytes. *J Mol Cell Cardiol*. 2005; 38(3):495–503. [PubMed: 15733909]
43. Gilbert TW, Sellaro TL, Badylak SF. Decellularization of tissues and organs. *Biomaterials*. 2006; 27(19):3675–83. [PubMed: 16519932]
44. Choi H, Nesvizhskii AI. False discovery rates and related statistical concepts in mass spectrometry-based proteomics. *Journal of proteome research*. 2008; 7(1):47–50.10.1021/pr700747q [PubMed: 18067251]
45. Kumar D, Hacker TA, Buck J, Whitesell LF, Kaji EH, Douglas PS, et al. Distinct mouse coronary anatomy and myocardial infarction consequent to ligation. *Coron Artery Dis*. 2005; 16(1):41–4. [PubMed: 15654199]
46. Singla DK, Hacker TA, Ma L, Douglas PS, Sullivan R, Lyons GE, et al. Transplantation of embryonic stem cells into the infarcted mouse heart: formation of multiple cell types. *J Mol Cell Cardiol*. 2006; 40(1):195–200. [PubMed: 16288779]
47. Trivedi P, Hematti P. Derivation and immunological characterization of mesenchymal stromal cells from human embryonic stem cells. *Experimental hematology*. 2008; 36(3):350–9.10.1016/j.exphem.2007.10.007 [PubMed: 18179856]
48. Fries KM, Blieden T, Looney RJ, Sempowski GD, Silvera MR, Willis RA, et al. Evidence of fibroblast heterogeneity and the role of fibroblast subpopulations in fibrosis. *Clin Immunol Immunopathol*. 1994; 72(3):283–92. [PubMed: 7914840]

49. Chang HY, Chi JT, Dudoit S, Bondre C, van de Rijn M, Botstein D, et al. Diversity, topographic differentiation, and positional memory in human fibroblasts. *Proc Natl Acad Sci U S A*. 2002; 99(20):12877–82. [PubMed: 12297622]
50. Lekic PC, Pender N, McCulloch CA. Is fibroblast heterogeneity relevant to the health, diseases, and treatments of periodontal tissues? *Crit Rev Oral Biol Med*. 1997; 8(3):253–68. [PubMed: 9260043]
51. Pflieger D, Chabane S, Gaillard O, Bernard BA, Ducoroy P, Rossier J, et al. Comparative proteomic analysis of extracellular matrix proteins secreted by two types of skin fibroblasts. *Proteomics*. 2006; 6(21):5868–79. [PubMed: 17068760]
52. Brizzi MF, Tarone G, Defilippi P. Extracellular matrix, integrins, and growth factors as tailors of the stem cell niche. *Current opinion in cell biology*. 2012; 24(5):645–51.10.1016/j.ceb.2012.07.001 [PubMed: 22898530]
53. Hynes RO. The extracellular matrix: not just pretty fibrils. *Science*. 2009; 326(5957):1216–9. [PubMed: 19965464]
54. Willems IE, Arends JW, Daemen MJ. Tenascin and fibronectin expression in healing human myocardial scars. *J Pathol*. 1996; 179(3):321–5.10.1002/(SICI)1096-9896(199607)179:3<321::AID-PATH555>3.0.CO;2-8 [PubMed: 8774490]
55. Konstandin MH, Toko H, Gastelum GM, Quijada PJ, De La Torre A, Quintana M, et al. Fibronectin is Essential for Reparative Cardiac Progenitor Cell Response Following Myocardial Infarction. *Circ Res*. 2013;10.1161/CIRCRESAHA.113.301152
56. Berger S, Dyugovskaya L, Polyakov A, Lavie L. Short-term fibronectin treatment induces endothelial-like and angiogenic properties in monocyte-derived immature dendritic cells: Involvement of intracellular VEGF and MAPK regulation. *European journal of cell biology*. 2012;10.1016/j.ejcb.2012.02.003
57. Ruoslahti E. Fibronectin and its receptors. *Annual review of biochemistry*. 1988; 57:375–413.10.1146/annurev.bi.57.070188.002111
58. Pankov R, Yamada KM. Fibronectin at a glance. *Journal of cell science*. 2002; 115(Pt 20):3861–3. [PubMed: 12244123]
59. Plow EF, Haas TA, Zhang L, Loftus J, Smith JW. Ligand binding to integrins. *J Biol Chem*. 2000; 275(29):21785–8.10.1074/jbc.R000003200 [PubMed: 10801897]
60. Bornstein P. Matricellular proteins: an overview. *Journal of cell communication and signaling*. 2009; 3(3–4):163–5.10.1007/s12079-009-0069-z [PubMed: 19779848]
61. Rifkin DB. Latent transforming growth factor-beta (TGF-beta) binding proteins: orchestrators of TGF-beta availability. *J Biol Chem*. 2005; 280(9):7409–12.10.1074/jbc.R400029200 [PubMed: 15611103]
62. Bujak M, Frangogiannis NG. The role of TGF-beta signaling in myocardial infarction and cardiac remodeling. *Cardiovasc Res*. 2007; 74(2):184–95.10.1016/j.cardiores.2006.10.002 [PubMed: 17109837]
63. Rabinovich GA, Sotomayor CE, Riera CM, Bianco I, Correa SG. Evidence of a role for galectin-1 in acute inflammation. *European journal of immunology*. 2000; 30(5):1331–9.10.1002/(SICI)1521-4141(200005)30:5<1331::AID-IMMU1331>3.0.CO;2-H [PubMed: 10820379]
64. Kuwabara I, Liu FT. Galectin-3 promotes adhesion of human neutrophils to laminin. *J Immunol*. 1996; 156(10):3939–44. [PubMed: 8621934]
65. Sano H, Hsu DK, Yu L, Apgar JR, Kuwabara I, Yamanaka T, et al. Human galectin-3 is a novel chemoattractant for monocytes and macrophages. *J Immunol*. 2000; 165(4):2156–64. [PubMed: 10925302]
66. McCurdy SM, Dai Q, Zhang J, Zamilpa R, Ramirez TA, Dayah T, et al. SPARC mediates early extracellular matrix remodeling following myocardial infarction. *Am J Physiol Heart Circ Physiol*. 2011; 301(2):H497–505.10.1152/ajpheart.01070.2010 [PubMed: 21602472]
67. Westermann D, Mersmann J, Melchior A, Freudenberger T, Petrik C, Schaefer L, et al. Biglycan is required for adaptive remodeling after myocardial infarction. *Circulation*. 2008; 117(10):1269–76.10.1161/CIRCULATIONAHA.107.714147 [PubMed: 18299507]

68. Freytes DO, Santambrogio L, Vunjak-Novakovic G. Optimizing dynamic interactions between a cardiac patch and inflammatory host cells. *Cells, tissues, organs*. 2012; 195(1–2):171–82.10.1159/000331392 [PubMed: 21996612]
69. Valentin JE, Stewart-Akers AM, Gilbert TW, Badylak SF. Macrophage participation in the degradation and remodeling of extracellular matrix scaffolds. *Tissue Eng Part A*. 2009; 15(7):1687–94.10.1089/ten.tea.2008.0419 [PubMed: 19125644]
70. Brown BN, Londono R, Tottey S, Zhang L, Kukla KA, Wolf MT, et al. Macrophage phenotype as a predictor of constructive remodeling following the implantation of biologically derived surgical mesh materials. *Acta Biomater*. 2012; 8(3):978–87.10.1016/j.actbio.2011.11.031 [PubMed: 22166681]
71. Badylak SF, Valentin JE, Ravindra AK, McCabe GP, Stewart-Akers AM. Macrophage phenotype as a determinant of biologic scaffold remodeling. *Tissue Eng Part A*. 2008; 14(11):1835–42.10.1089/ten.tea.2007.0264 [PubMed: 18950271]
72. Terrovitis J, Lautamaki R, Bonios M, Fox J, Engles JM, Yu J, et al. Noninvasive quantification and optimization of acute cell retention by in vivo positron emission tomography after intramyocardial cardiac-derived stem cell delivery. *J Am Coll Cardiol*. 2009; 54(17):1619–26. 10.1016/j.jacc.2009.04.097 S0735-1097(09)02505-4. [pii]. [PubMed: 19833262]
73. Bonios M, Terrovitis J, Chang CY, Engles JM, Higuchi T, Lautamaki R, et al. Myocardial substrate and route of administration determine acute cardiac retention and lung bio-distribution of cardiosphere-derived cells. *Journal of nuclear cardiology : official publication of the American Society of Nuclear Cardiology*. 2011; 18(3):443–50.10.1007/s12350-011-9369-9 [PubMed: 21448759]
74. Terrovitis JV, Smith RR, Marban E. Assessment and optimization of cell engraftment after transplantation into the heart. *Circ Res*. 2010; 106(3):479–94.10.1161/CIRCRESAHA.109.208991 [PubMed: 20167944]
75. Zimmermann WH, Melnychenko I, Wasmeier G, Didie M, Naito H, Nixdorff U, et al. Engineered heart tissue grafts improve systolic and diastolic function in infarcted rat hearts. *Nat Med*. 2006; 12(4):452–8. [PubMed: 16582915]
76. Vunjak-Novakovic G, Tandon N, Godier A, Maidhof R, Marsano A, Martens TP, et al. Challenges in cardiac tissue engineering. *Tissue engineering Part B, Reviews*. 2010; 16(2):169–87.10.1089/ten.TEB.2009.0352 [PubMed: 19698068]
77. Wei HJ, Chen CH, Lee WY, Chiu I, Hwang SM, Lin WW, et al. Bioengineered cardiac patch constructed from multilayered mesenchymal stem cells for myocardial repair. *Biomaterials*. 2008; 29(26):3547–56.10.1016/j.biomaterials.2008.05.009 [PubMed: 18538386]
78. Dvir T, Kedem A, Ruvinov E, Levy O, Freeman I, Landa N, et al. Prevascularization of cardiac patch on the omentum improves its therapeutic outcome. *Proc Natl Acad Sci U S A*. 2009; 106(35):14990–5.10.1073/pnas.0812242106 [PubMed: 19706385]
79. Giraud MN, Ayuni E, Cook S, Siepe M, Carrel TP, Tevæarai HT. Hydrogel-based engineered skeletal muscle grafts normalize heart function early after myocardial infarction. *Artificial organs*. 2008; 32(9):692–700.10.1111/j.1525-1594.2008.00595.x [PubMed: 18684206]
80. Godier-Furnemont AF, Martens TP, Koeckert MS, Wan L, Parks J, Arai K, et al. Composite scaffold provides a cell delivery platform for cardiovascular repair. *Proc Natl Acad Sci U S A*. 2011; 108(19):7974–9.10.1073/pnas.1104619108 [PubMed: 21508321]

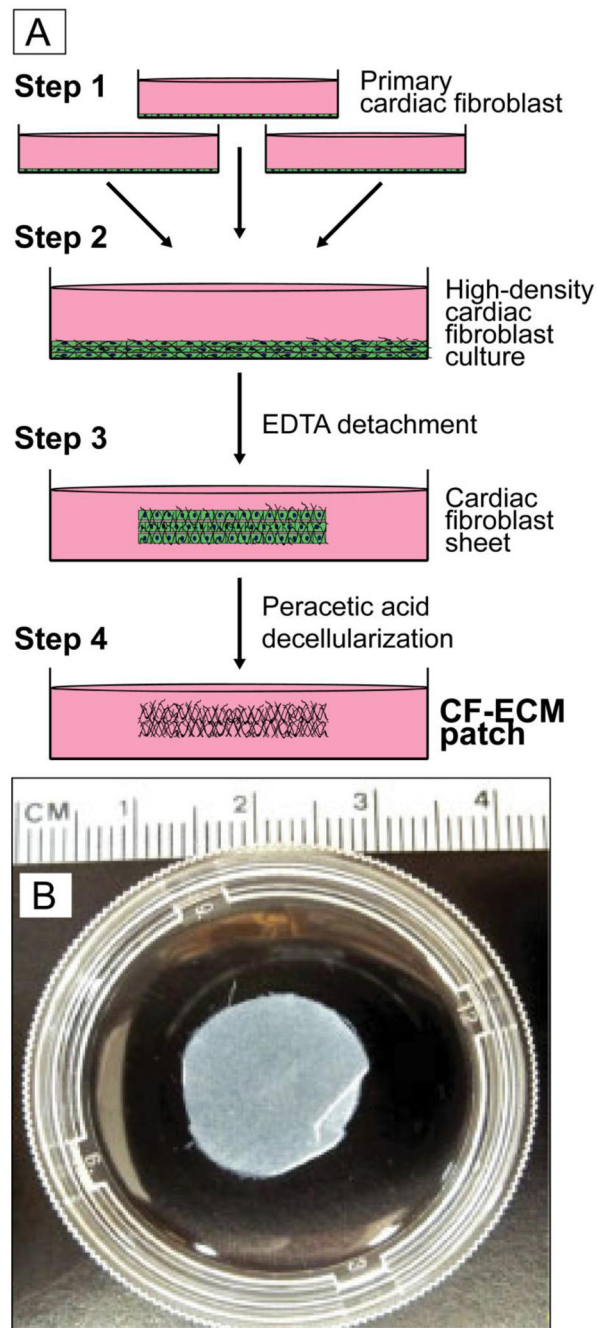


Figure 1.
A CF-ECM production method. B) Representative decellularized CF-ECM scaffold, approximately 16 mm in diameter.

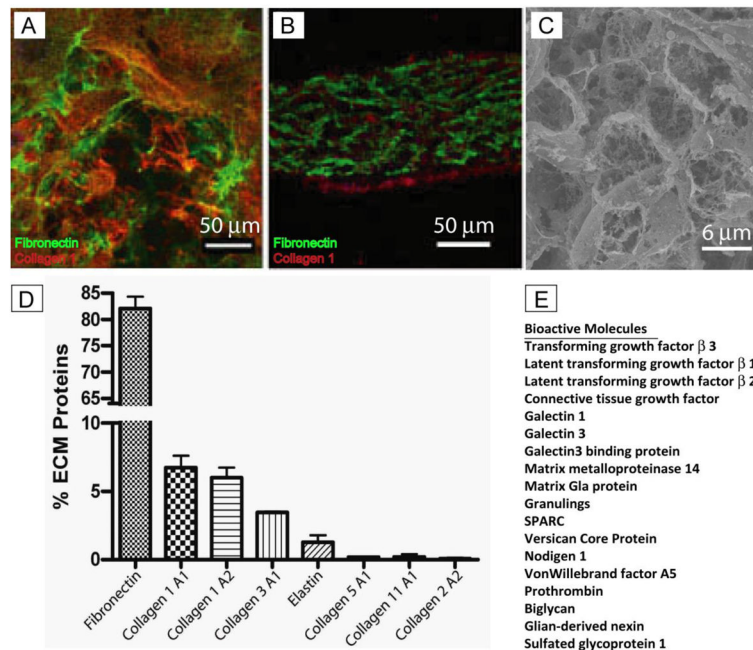


Figure 2.

A, Surface staining of CF-ECM scaffold (scale bar = 50 μ m). B, Cross section of CF-ECM scaffold, note the thickness of approximately 150 μ m, Fibronectin (green), Collagen type I (red), DAPI (blue) (scale bar = 50 μ m). C, Scanning electron micrograph of CF-ECM surface (scale bar = 40 μ m). Note the absence of DAPI staining in the scaffolds, indicating the absence of residual cells. D) Protein composition of the CF-ECM scaffold. Note the high fibronectin content. E) Bioactive molecules identified by mass spectrometry

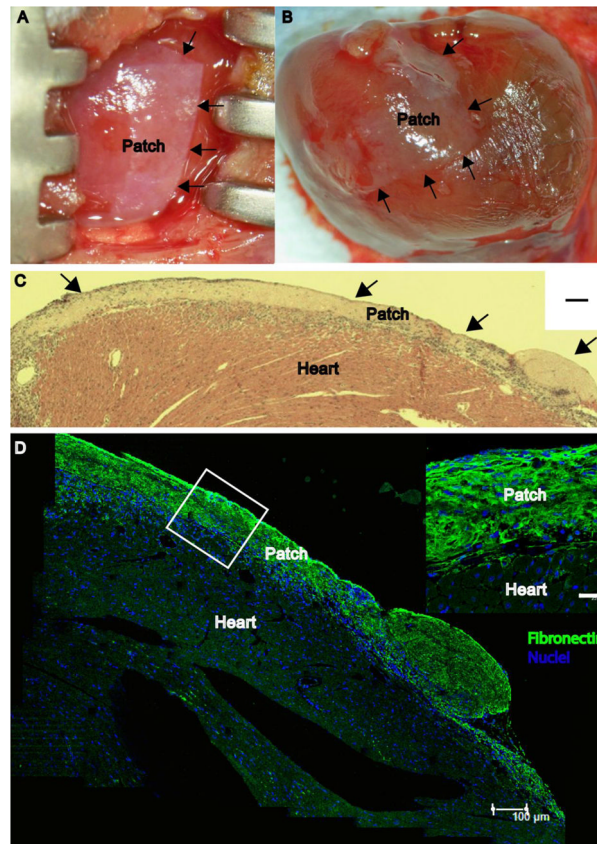


Figure 3.

A, CF-ECM at time of placement on the mouse heart (0 h), arrows denote the edge of the scaffold. B, Attached scaffold after 48 h the beating mouse heart, arrows denote the edge of the scaffold. C, Hematoxylin and eosin stain of a cross-section of the epicardial surface, arrows denote the scaffold. Note the absence of gaps between the scaffold and epicardial surface (scale bar = 100 μ m) confirming adherence. D, Immunofluorescent micrograph of an attached scaffold after 48 hours on the beating mouse heart (scale bar = 100 μ m). Inset image denotes the tight attachment between CF-ECM scaffold and the epicardial surface. Fibronectin (green), DAPI (Blue) (scale bar = 25 μ m).

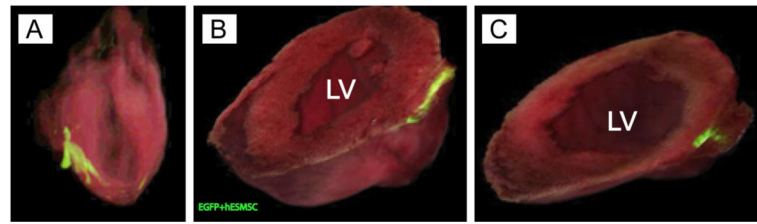


Figure 4.

A, Long axis view of three dimensional whole heart image reconstructions of co-registered bright field and confocal images. B) Short axis view approximately half way from apex to base, C) Short axis view toward apex of the heart. Note the infiltration of EGFP+hMSC into the epicardial surface just under the patch. Green = CF-ECM bioscaffold seeded with EGFP +hMSCs, LV= left ventricle.

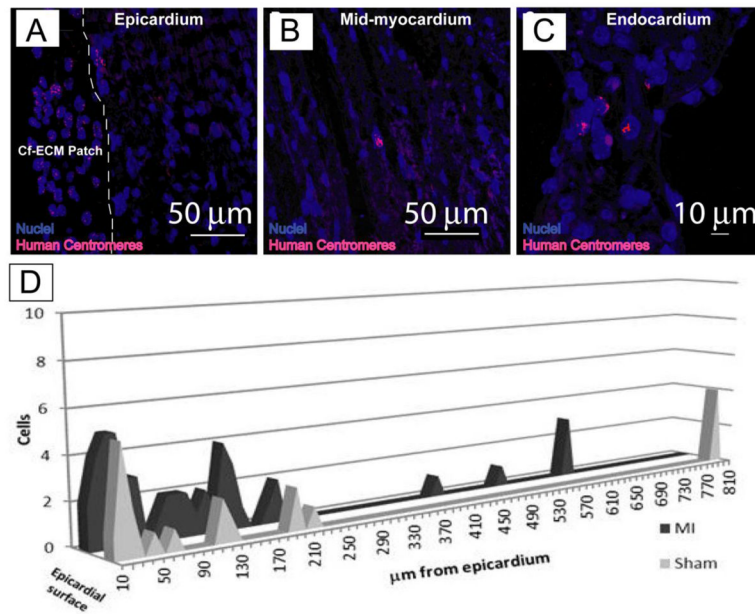


Figure 5.

FISH staining for human centromeres (pink), Nuclei (blue) indicates the presence of human cells within the infarcted mouse heart. Note that cardiomyocytes (purple) are highly autofluorescent helping to distinguish hEMSCs from myocytes. A, the epicardial surface with attached scaffold, note the presence of hEMSCs in the CF-ECM scaffold. The dashed line indicates the interface between the CF-ECM scaffold and the epicardium (scale bar = 50 μm). B, Mid-myocardium with human nuclei (scale bar = 50 μm). C, endocardial surface with human nuclei present (scale bar = 10 μm). D) Cumulative numbers of human nuclei in a single heart slice from each animal tested (treated n=8, sham n=3) and the distance from the epicardial surface the cells were observed. Note that cell transfer was observed in both MI and sham animals, indicating that hEMSC can migrate in the absence of an injury signal. Scaffolds were seeded with 7.5×10^5 cells.